TRAVELING WAVE FAULT LOCATION TECHNOLOGY FOR DISTRIBUTION NETWORK LINES BASED ON IMPROVED SPARROW SEARCH ALGORITHM

*Xing Xiao[1], Chenxu Meng[1], Lingcheng Zeng[1], Qiang Zhou[2]**
[1]China Southern Power Grid Guangdong Zhongshan Power Supply Bureau, Zhongshan, 528400, China
[2]College of Electrical and Electronic Engineering, Shandong University of Technology, Zibo, 255000, China

Abstract - Traveling wave fault location (TWFL) in distribution networks is crucial for grid reliability. To more accurately detect the location of faults in distribution network lines, the paper proposes an improved sparrow search algorithm (ISSA), introducing Torus sequence and random walk strategy, and improving the individual position update formula. The new TWFL method is proposed by combining the ISSA with the variational mode decomposition algorithm. The experiment demonstrated that the improved algorithm had good convergence performance and could fully converge in Sphere, SumSquares, and Ackley test functions, with average results of 4.45E-24, 3.95E-37, and 2.15E-32. Compared with similar methods, the proposed ranging method had the smallest ranging error, with an error rate of only 0.5%. The research method has good detection performance in TWFL of distribution networks, providing a certain reference value for the field of distribution network fault detection.

Keywords: Sparrow search algorithm; VMD algorithm; Traveling wave fault location; Distribution network; Fault detection.

1. Introduction

The increasing demand for electricity and the acceleration of urbanization have made the complexity and importance of the Distribution Network (DNet) increasingly apparent. As the last link in the power system, DNet is crucial in the transmission and distribution of electrical energy. However, DNet cannot avoid faults during operation, such as short circuits, grounding faults, and other accidents, which affect the reliability of the power supply and may cause huge economic losses and safety hazards [1-2]. Therefore, quickly and accurately locating the fault point is vital for guaranteeing the secure operation of DNet. Traveling Wave Fault Location (TWFL) technology has become an important method for DNet fault localization since its high precision and fast response advantages [3-4]. Many scholars have conducted extensive research on TWFL technology for DNet transmission lines. Jnaneswar et al. proposed a novel multi-terminal non-uniform AC microgrid fault location method to address the bidirectional power flow problem caused by the penetration of distributed generation. This method outperformed traditional traveling wave-based methods in terms of performance [5]. Zhang et al. proposed a detection method built on enhanced Variational Mode Decomposition (VMD) to address the cross-term problem of Wigner-Ville distribution in detecting fault traveling waves. This method was faster and more accurate than the wavelet and Hilbert-Huang transform [6]. Zeng et al. put forward a feature extraction strategy built on successive VMD and Teager energy operator for the TWFL problem of multi-terminal transmission lines, and obtained feasible and reliable test results [7].

Other intelligent algorithms also have certain applications in DNet fault detection. Ni et al. proposed a fusion strategy that fuses adaptive moving average, SVM, and the Improved Sparrow Search Algorithm (ISSA) to address the issue of traditional commodity trading advisory strategies relying on fixed technical indicators. This strategy achieved an annualized return rate of 18% and high F1 scores across multiple market cycles [8]. Wang et al. proposed an ISSA to address the issues of insufficient fitting accuracy and low computational efficiency in traditional feedback neural network agent models. Combined with an enhanced Backpropagation (BP) neural network, it significantly improved the fitting accuracy [9]. Xue et

https://doi.org/10.17683/ijomam/issue22.v2.9

al. proposed a new enhanced SSA to address the insufficient search capability in SSA, significantly improving convergence accuracy. This algorithm achieved an absolute percentage error of 1.2778% and a root mean square error of 1.2171 in short-term load forecasting [10]. Wei et al. developed a Grounding Fault Line Selection (GFLS)method built on ISSA to address insufficient utilization of transient power frequency current components during single-phase grounding faults in high-voltage grounding systems, which had high reliability and strong robustness [11]. The traditional BP model has problems such as insufficient fitting accuracy and low computational efficiency. Therefore, Wang J et al. proposed an ISSA-BP method that integrates BP and ISSA, and optimized the reliability calculation of the BP network by introducing the golden sine strategy and opposition learning strategy. The experimental results showed that this method significantly improved the fitting accuracy while maintaining the computational efficiency. Its effectiveness in structural reliability analysis has been verified through a case study of metro bogies [12]. Long-distance transmission line fault traveling wave heads have problems such as low detection accuracy, unsynchronized fault detection equipment clocks, and position deviation caused by uncertain traveling wave speed. In view of this, Zhou J et al. proposed a new fault location method based on a combination of improved VMD and Teager-Kaiser Energy Operator (TKEO). This method optimized the VMD parameters, decomposed the linear mode and zero mode components of the fault traveling wave, and used TKEO to detect the wave head. Then, based on the time difference between the wave heads arriving at the measuring point, a double-ended traveling wave positioning formula that was independent of timing and wave speed is derived. The simulation results showed that this method had good applicability under noise and different ground resistances and fault types, and the accuracy of the positioning results was high [13]. Nazeer S K et al. proposed a method based on Discrete Wavelet Transform (DWT) for the problem of fault location in multi-port transmission lines. This method could accurately identify faults between terminal lines or access points and effectively reduce computational overhead. The arrival time of the subsequent wave peaks caused by the fault was determined through the traveling wave theory, thereby accurately calculating the fault location. The experimental results showed that this method demonstrated good effectiveness under different fault types, fault resistances, and fault initiation angles, and its applicability has been verified in the integrated renewable energy power grid [14].

In current research, although DNet TWFL technology has achieved many results, there are still some shortcomings. Firstly, there is still room for improvement in the precision of fault location using existing ranging methods. Secondly, many studies rely on fixed technical indicators and complex models, resulting in insufficient robustness of algorithms and difficulty in adapting to different application scenarios. To overcome the above shortcomings, the paper proposes an ISSA. This algorithm combines the Torus sequence and Random Walk Strategy (RWS) to update and optimize individual positions, enhancing the search capacity and convergence velocity. Meanwhile, the improved algorithm is combined with VMD to form a new TWFL method. The innovation mainly lies in using the low difference sequence of the Torus sequence to improve the distribution of SSA in the initialization stage, introducing logarithmic decreasing inertia weight and RWS. The combination of these strategies effectively prevents premature convergence.

2. Methods and Materials

2.1 Application of TWFL Technology for DNet Lines based on ISSA

TWFL technology mainly relies on the propagation characteristics of fault waves in power lines and uses the current or voltage waveforms measured by sensors to calculate the location of the fault occurrence. SSA can reduce distance measurement errors in complex power grid structures and multiple types of faults. Therefore, this study will explore the application of SSA in TWFL technology. SSA is a novel algorithm that simulates the sparrows' foraging behavior to achieve efficient global optimization. Although SSA has fast convergence and strong optimization capabilities, it still has shortcomings. Firstly, population initialization based on chaotic mapping may lead to concentration of individual distributions, thereby affecting convergence performance. Secondly, the individual update formula did not take into account the influence of weights on the convergence process. Finally, the lack of perturbation strategies makes the algorithm prone to dropping into local optima. To this end, improvement methods include optimizing population initialization, updating individual position formulas, and introducing perturbation strategies. The population is segmented into discoverers, followers, and scouts to enhance global search capabilities. The Position Update Strategy (PUS) formula of the discoverer is given by Eq. (1).

$$x_{ij}^{t+1} = \begin{cases} x_{ij}^{t} \cdot \exp(\frac{-i}{\varepsilon \cdot MaxCycle}), R_2 < ST \\ x_{ij}^{t} + P \cdot E, R_2 \geq ST \end{cases} \quad (1)$$

In Eq. (1), x_{ij}^{t} means the position of sparrow i in dimension j after t iterations. *MaxCycle* is the maximum iteration for the population. ε is a random number with a value range of $[0,1]$. ST is the safety threshold, and R_2 is the alert value. P is a random number under normal distribution. E is the identity matrix. In DNet fault location, the discoverer continuously adjusts their own position to better approach the location of the fault point, and improves the precision of fault localization by guiding the search process. Followers follow the discoverer and conduct fine searches within the local area discovered by the discoverer. The PUS of followers is given by Eq. (2).

$$x_{ij}^{t+1}=\begin{cases} P\cdot\exp(\dfrac{x_{wj}^{t}-x_{ij}^{t}}{i^{2}}), i>\dfrac{n}{2} \\ x_{Fj}^{t+1}+\left|x_{ij}^{t}-x_{Fj}^{t+1}\right|\cdot A^{+}\cdot E, i\le\dfrac{n}{2} \end{cases} \tag{2}$$

In Eq. (2), x_{Fj}^{t} is the optimal location for followers after t iterations. x_{wj}^{t} means the worst position of the population after t iterations. x_{uj}^{t} denotes the generalized inverse matrix of A. n is the population size of sparrows. Investigators are responsible for monitoring hazardous factors in the environment. When danger is perceived, the investigator issues an alert to the population, which triggers an anti predator mechanism to quickly flee the current area to prevent the population from falling into local optima and enhance population diversity. The PUS calculation of the investigator is expressed in Eq. (3).

$$x_{ij}^{t+1}=\begin{cases} x_{ij}^{t}+\left|x_{ij}^{t}-x_{bj}^{t}\right|\cdot\lambda, f_i\neq f_b \\ x_{ij}^{t}+\dfrac{\left|x_{ij}^{t}-x_{wj}^{t}\right|}{(f_i-f_w)+c}\cdot\rho, f_i=f_b \end{cases} \tag{3}$$

In Eq. (3), x_{bj}^{t} is the global optimal position after t iterations. λ is the step size control parameter that conforms to the standard normal distribution. ρ is a random number within $[-1,1]$. c is a small constant to prevent the denominator from being 0. f_i refers to the current fitness, f_b denotes the global optimal fitness, and f_w means the global worst fitness. The specific process of TWFL technology for DNet lines based on ISSA is shown in Fig.1.

In Figure 1, the application of ISSA in DNet line TWFL technology improves the dispersion of fault location solutions through a novel population initialization method, aiming to explore the search space more comprehensively. The algorithm classifies the population into discoverers, followers, and scouts, responsible for global search, local optimization, and detection of local optimal solutions for fault locations, respectively. After evaluating the fitness, the algorithm iteratively optimizes and ultimately outputs precise fault location estimates, thereby enhancing the safety of the power grid.

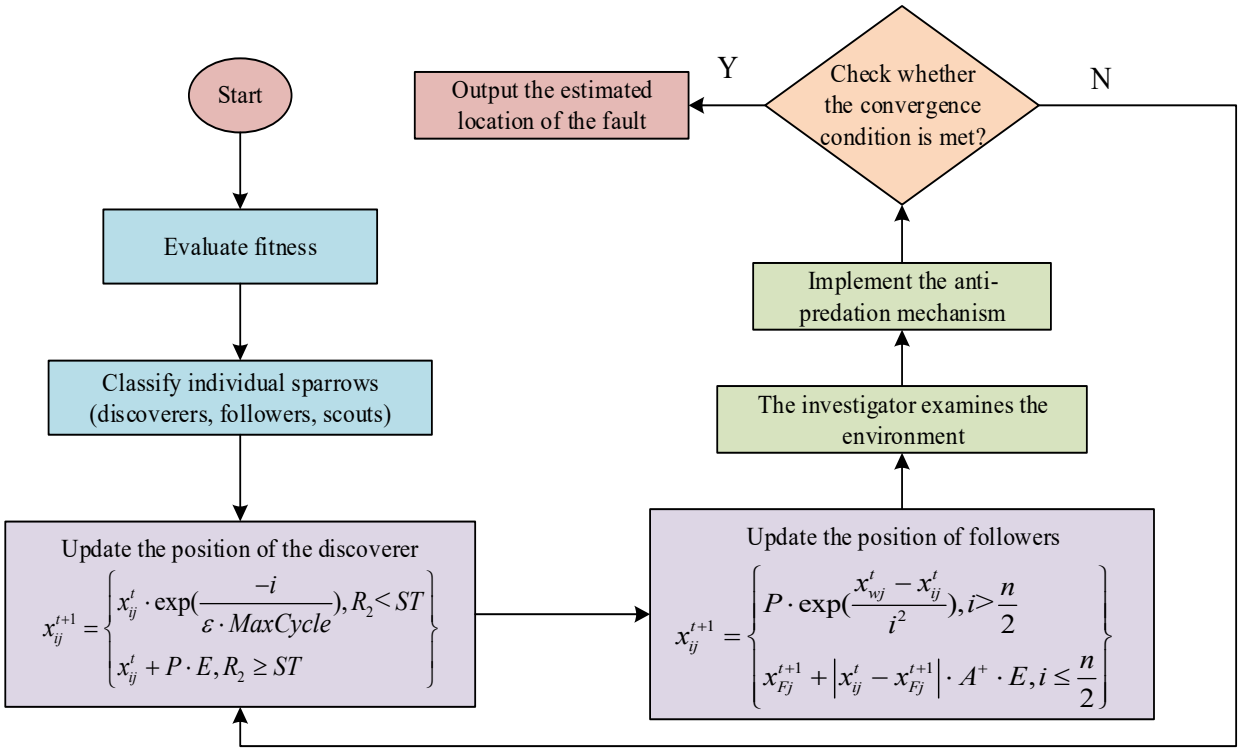

Figure 1: Flowchart of the TWFL technology for DNet lines based on ISSA

2.2 Population Initialization and Individual PUS based on ISSA

After introducing the application of TWFL technology for DNet lines based on ISSA, to further improve the SSA's performance, it is necessary to research population initialization and individual PUS. Therefore, this study will explore improved population initialization methods and PUS to enhance the overall convergence and search efficiency. To improve the distribution of the initialized population in the model, this study uses the low difference sequence method instead of chaotic mapping to initialize the population [15]. The Torus sequence, as a novel low difference sequence based on prime sequences, has the advantage of a more uniform distribution compared to other common sequences. Therefore, this study adopts the Torus sequence as an improved population initialization method. The expression of the Torus sequence is given by Eq. (4) [16].

$$\alpha_k = (f(k\sqrt{s_1}, k\sqrt{s_2}, \cdots k\sqrt{s_d}) \tag{4}$$

In Eq. (4), $f(x) = x - [x]$, k is the current iteration times of the population, and s_d is a randomly generated prime sequence. The Torus sequence maps a randomly generated prime sequence to the $[0,1)$ interval through square root and rounding functions. By squaring the prime sequence, the diversity of the sequence is preserved, thereby ensuring the distribution of the population initialized through the Torus sequence. By rounding the function, the generated result is rounded to zero, reducing the differences between randomly generated prime sequences. The initial position of the population individuals initialized through the Torus sequence is shown in Eq. (5).

$$x_i = x_{\min} + \alpha_i (x_{\max} - x_{\min}) \tag{5}$$

In Eq. (5), $x_{\min}$ and $x_{\max}$ are the min and max of the global solution space of the population. α_i is the i-th uniformly distributed low variance random number generated by the Torus sequence within the $[0,1]$-interval. The convergence speed of swarm algorithms is influenced by the collaboration between individuals and groups. When an individual finds a good position, the cooperative mechanism prompts the entire group to approach that position, helping to achieve the optimal solution.

However, in SSA, followers have a strong tendency towards discoverers, leading to most individuals clustering around local optima and potentially missing out on global optima. Introducing inertia weight can improve this problem. In the early stage of iteration, the inertia weight is reduced rapidly and slowly reduced in the later stage of iteration, helping the group to quickly find a good solution in the early stage of iteration. In the later stages of the iteration, detailed local searches are performed to avoid missing the global optimal solution. Therefore, this study adopts logarithmic decreasing inertia weights, as shown in Eq. (6).

$$w(t) = w_{\max} - \mu(w_{\max} - w_{\min}) \log_{MaxCycle} t \tag{6}$$

In Eq. (6), w is the inertia weight, which can be relatively large in the early stages of the algorithm to encourage individuals to explore the solution space faster, and gradually decrease in the later phases to enable individuals to search more carefully for regions close to the optimal solution. $w_{\max}$ is the maximum value of inertia weight, and its impact on DNet fault diagnosis is that it can promote rapid adaptation to new fault scenarios and improve the timeliness of fault identification. $w_{\max}$ is the minimum value, which ensures that individuals reduce the exploration amplitude at appropriate time points and focus on refining local solutions, thereby improving the diagnostic accuracy of fault types and locations. μ is the logarithmic adjustment coefficient. After introducing inertia weights, the location update formula improved by the discoverer is given by Eq. (7).

$$x_{ij}^{t+1} = \begin{cases} wx_{ij}^t, R_2 < ST \\ x_{ij}^t + P \cdot E, R_2 \geq ST \end{cases} \tag{7}$$

SSA lacks mutation and perturbation strategies, which can easily lead to premature convergence of the algorithm. If Gaussian and Cauchy mutation operators are introduced as mutation strategies in SSA, it will increase the computational complexity. Meanwhile, the mutation operator can also affect the convergence velocity and precision of the algorithm [17]. This study introduces an RWS as a perturbation strategy in SSA to enhance the algorithm's global optimization capability. The RWS process is displayed in Fig. 2.

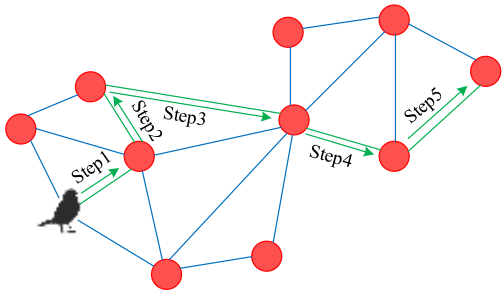

Figure 2: Schematic diagram of RWS

In Fig.2, in this process, individuals explore the solution space through random walks to avoid premature convergence caused by the attraction of local optimal solutions. The design of random walk steps introduces a certain number of random step sizes, allowing individuals to flexibly deviate from their current position in each iteration, thereby expanding the search range and increasing the diversity of solutions. The mathematical expression of the random walk process is shown in Eq. (8).

$$X(t)=\begin{bmatrix}0, cumsum(2r(t_1)-1), cumsum(2r(t_2)-1), \cdots, \\ cumsum(2r(t_n)-1)\end{bmatrix} \quad (8)$$

In Eq. (8), $X(t)$ is the set of random walk steps. In fault diagnosis, an appropriate number of steps can help individuals jump out of possible local optima and explore a broader solution space, thereby improving their ability to detect and locate faults. $cumsum$ is for calculating the cumulative sum. This accumulation process can make individuals more flexible in exploring the solution space and better adapt to changing fault situations, achieving dynamic adjustment. t_n is the number of random walk steps. Compared to a fixed step size, changing the number of steps can increase the randomness of individuals, which helps to avoid premature convergence in the optimization process.

2.3 DNet TWFL Combining ISSA and VMD

After exploring the population initialization and individual PUS of ISSA, this study will focus on how to combine ISSA with VMD to achieve more efficient Traveling Wave Fault (TWF) detection. VMD is an excellent detection method that can be used as a signal decomposition method for decomposing and processing TWF information [18]. The number of modes, penalty parameters, initialization mode, and other parameters in VMD can be set by users themselves to meet different signal processing requirements. Therefore, this study introduces ISSA into VMD to find the optimal combination of two key parameters, the number of modes and the penalty factor, through ISSA, to improve VMD's performance. The process of VMD after introducing ISSA is shown in Fig.3.

In Figure 3, the process of VMD can be roughly separated into 4 stages: signal acquisition, parameter combination optimization, traveling wave head calibration, and fault location. The first step is to determine the relevant parameters and sampling frequency of the DNet line, and use the Karen Bell transform method on the collected current waveform to obtain the line mode component.

The next step is to set the ISSA parameters and initialize them. To obtain the best combination of parameters, the fitness function of ISSA is set as relative entropy, with the goal of obtaining the minimum relative entropy, that is, obtaining the sub-data column with the highest similarity to the original data column. Before calculating relative entropy, the original signal needs to be processed through the Hilbert transform. The expression of the Hilbert transform is given by Eq. (9).

$$H\left[x_K(t)\right]=\frac{1}{\pi}\int_{-\infty}^{\infty}\frac{x_K(\tau)}{t-\tau}d\tau \quad (9)$$

In Eq. (9), $x_K(\tau)$ is the original signal. $H\left[x_K(t)\right]$ is the signal after Hilbert transform. t is the time point. Next, all Intrinsic Mode Function (IMF) components after VMD decomposition are extracted and normalized, as shown in Eq. (10).

$$\hat{A}_K(t)=\frac{\left|H\left[x_K(t)\right]\right|}{\sum_t\left|H\left[x_K(t)\right]\right|} \quad (10)$$

In Eq. (10), $\hat{A}_K(t)$ represents the normalized result. Finally, the relative entropy values of all IMF components are accumulated to obtain the relative entropy corresponding to the individual's current position. The absolute entropy calculation formula is shown in Eq. (11).

$$S_i=-\sum_t\hat{A}_K(t)\log(\hat{A}_K(t)) \quad (11)$$

In Eq. (11), S_i is the relative entropy of the i-th individual. After calculating the relative entropy of all individuals, the positions and relative entropy of paired individuals are temporarily stored as the global optima of the population. After the initialization of ISSA is finished, the next step is to find the individual with the smallest relative entropy in the population, which is the globally optimal individual. The parameters corresponding to this individual are the optimal parameter combination. Then, VMD processes the Traveling Wave Signal (TWS) through the optimal parameter combination, calibrates the wavefront of the TWS, and finds the fault point. Finally, this study obtains the fault distance using the double ended TWFL method, as shown in Fig. 4.

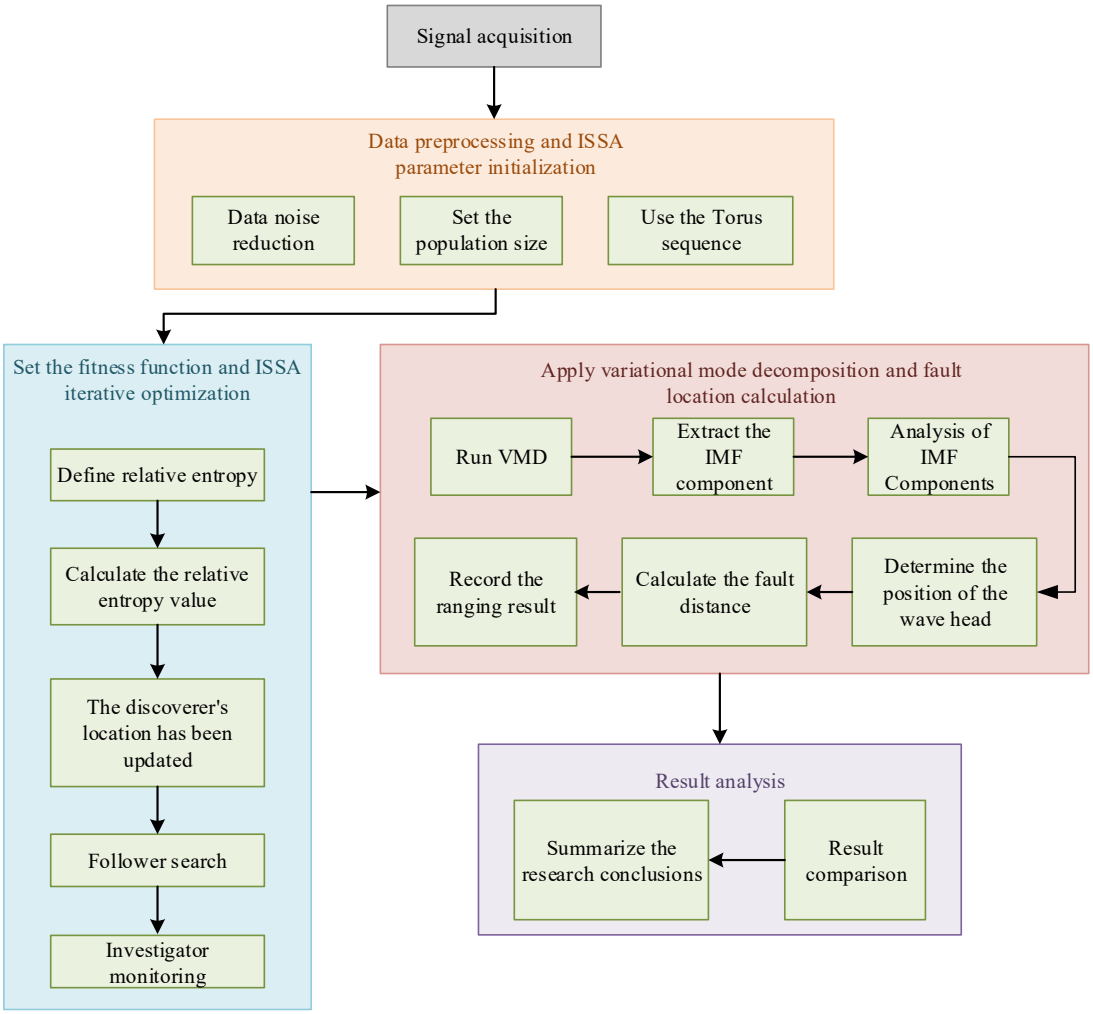

Figure 3: Flowchart of TWFL of DNet based on ISSA-VMD

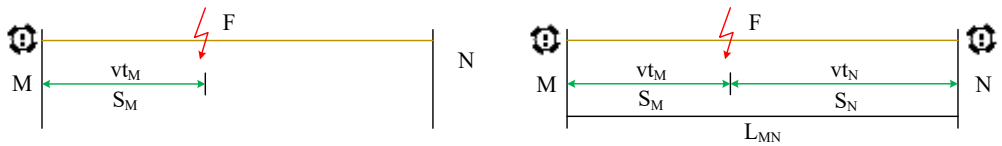

(a) Single ended traveling wave ranging (b) Dual terminal traveling wave ranging

Figure 4: TWFL method

Figures 4 (a) and (b) show single-ended and double-ended traveling wave ranging methods. The former has a low detection cost and fast positioning speed, but is not suitable for circuits with complex topology structures. Therefore, this study selects dual-end ranging. This method has high positioning precision, strong anti-interference ability, and is more suitable for fault detection of DNet lines with complex network topology structures.

3. Results

3.1 Performance Testing and Analysis of ISSA

To validate the effectiveness of the improved method, this study conducts experiments from two aspects: population initialization and random walk of the algorithm. To test the convergence performance of ISSA, it is compared with others. Comparative algorithms include SSA, Particle Swarm Optimization (PSO), and Improved PSO (IPSO). The testing functions include the unimodal testing functions Sphere and SumSquares, as well as the multimodal testing functions Ackley and Griebank. To ensure accuracy, the population size of each algorithm is 30, with a maximum iteration of 400. The remaining individual algorithm parameters are set to default values. The Torus sequence is compared with other common population initialization methods, including Circle mapping, Sobol sequence, and Sine mapping. The distribution maps generated by the four initialization methods are shown in Fig.5.

In Figure 5 (a), the population generated by the Torus sequence has the best distribution, with uniform population distribution and no individual

overlap. In Figure 5 (b), the population distribution generated by Circle mapping is poor, and there is a significant degree of individual overlap in the population. In Figures 5 (c) and (d), the population distribution generated by the Sobol sequence and Sine mapping is good. Among them, the individual overlap of Sobol sequences is relatively small, the population distribution is not uniform, and there are large blank areas in the population space that have not been distributed. The population distribution mapped by Sine is more uniform, with smaller blank areas but more individual overlap. To further compare the distribution of populations generated by Torus sequences, the distribution histograms of populations generated by Torus sequences and Sobol sequences are compared. The distribution histograms of the two sequences are shown in Fig.6.

In Figure 6 (a), the population generated by the Torus sequence has a uniform distribution. Individuals are distributed throughout almost the entire range of values, and the difference between the lowest and highest distribution frequencies is not significant, with quantities ranging from 20 to 30. In Fig.6 (b), the individual distribution of the population generated by the Sobol sequence varies greatly.

There are obvious individual non-distribution areas within the value range, with a quantity distribution range of 3 to 35. In the distribution area, the number of individuals with different values also varies greatly. Among them, there is a difference of 68 between the frequency with the highest individual distribution and the frequency with the lowest individual distribution. At the same time, the individuals of Sobol sequences are mainly distributed in the middle region, with fewer individuals on both sides of the range, making it difficult for the population to search for the edge regions of the space in subsequent iterations, thereby affecting the performance. In summary, the population generated through Torus sequence initialization has the best distribution and the best spatial traversal effect for individual populations. The results of the RWS are shown in Fig. 7.

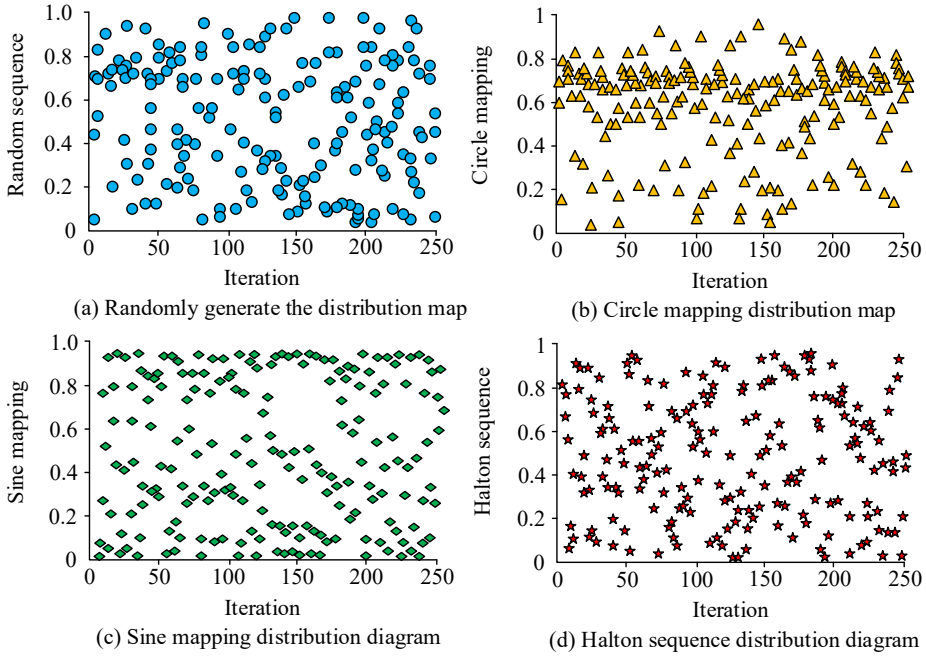

(a) Randomly generate the distribution map (b) Circle mapping distribution map

(c) Sine mapping distribution diagram (d) Halton sequence distribution diagram

Figure 5: Distribution generated by different initialization methods

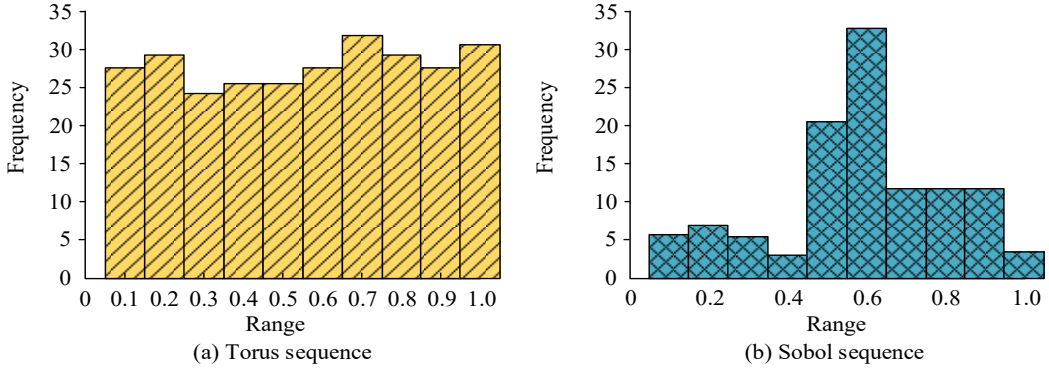

(a) Torus sequence (b) Sobol sequence

Figure 6: Distribution histograms of populations generated by Torus and Sobol sequences

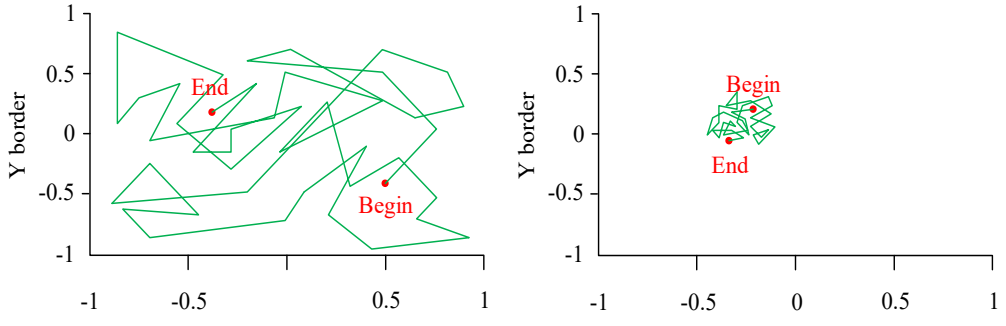

(a) Trajectory plot of random walk with maximum step size 0.5

(b) Trajectory plot of random walk with maximum step size 0.05

Figure 7: Comparison of RWS results

Table 1. Performance of different algorithms

Test unction	Result	SSA	ISSA	PSO	IPSO
Sphere	Mean	7.03E-26	4.45E-24	4.01E-12	2.80E-16
	Optima	0	0	4.69E-34	3.15E-46
SumSquares	Mean	6.34E-13	3.95E-37	9.84E-16	7.45E-16
	Optima	1.35E-33	0	2.06E-46	6.87E-31
Ackley	Mean	8.34E-28	2.15E-32	4.44E-22	3.23E-21
	Optima	0	0	3.64E-28	4.70E-26
Griewank	Mean	2.56E-37	1.64E-33	5.46E-24	6.71E-27
	Optima	7.58E-54	3.15E-49	1.61E-31	1.07E-29

In Figure 7 (a), when the maximum step size is 0.5, after random walks, the individual basically covers the entire space, corresponding to the early fast optimization ability. In Fig. 7 (b), when the maximum step size is 0.05, the individual's random walk will be limited to a small area, corresponding to the algorithm's ability to conduct detailed searches in the local space in the later stage. The RWS combines the global and local search capacities, enabling SSA to quickly survey global excellent positions in the early stages while improving its ability to develop local excellent positions in the later stages. Table 1 shows the test results of ISSA and other algorithms.

Table 1 shows the average and optimal values of each algorithm after 40 experiments. In the unimodal test function, PSO and IPS do not reach the theoretical optimal values, SSA only converges in the Sphere function, while ISSA reaches the theoretical optimal values in both Sphere and SumSquares, demonstrating better convergence accuracy. For the multimodal test function Ackley, SSA and ISSA can all find the global optima, while PSO and IPSO fall into local optima, indicating that SSA has stronger global optimization ability. In the multimodal test function Griebank, although none of the four algorithms find the theoretical optimal value, the average value of ISSA is lower than other algorithms, indicating its advantages in global search accuracy and stability. The optimal iterative convergence curve of the intelligent optimization algorithm in the Sphere and SumSquares test functions is shown in Fig. 8.

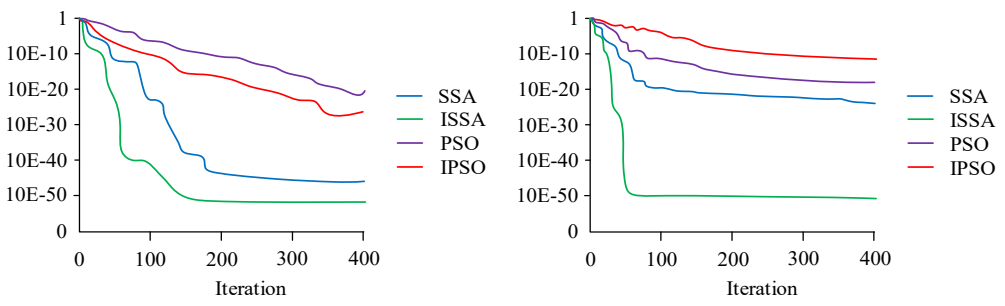

(a) Sphere iteration curve plot

(b) SumSquares iteration curve plot

Figure 8: Optimal iterative convergence results of different algorithms in Sphere and SumSquares test functions

In Figure 8 (a), ISSA approaches convergence in less than 100 iterations and fully converges in 150 iterations. SSA fully converges after 200 iterations. PSO and IPSO do not fully converge within the

specified number of iterations. In Fig.8 (b), ISSA fully converges in less than 100 iterations. SSA, PSO, and IPSO have not fully converged.

3.2 ISSA-VMD Fault Location Analysis

To test the fault location performance of VMD with ISSA, the paper focuses on a 10kV simulated DNet system and conducts comparative experiments with other algorithms such as VMD, SSA-VMD, VMD-TEO, and VMD-LSTM. The simulation software is ATP, the setting range of modal components is, and the setting range of penalty facto $[2,10]$ rs is $[100,2000]$. The parameters of ISSA are consistent with the above experiment. The waveform diagram of the three-phase current at fault F obtained by sampling at one of the collection points N of ISSA-VMD is shown in Fig. 9.

Figure 9 shows the waveform of a single-phase grounding fault at point F. The current amplitude of fault phase A undergoes a sudden change, but the magnitude of the change is relatively small. Non-faulty phases B and C are affected by electromagnetic coupling and also exhibit slight oscillations. The time for the N-terminal to receive fault information is about 0.05 seconds. The IMF components of the fault signal after phase mode transformation and decomposition are shown in Fig. 10.

Figure 10 shows the four IMF component diagrams of the processed fault signal. Figures. 10 (a) to (c) mainly show high-frequency noise and secondary oscillation components. In Fig. 10 (d), the wavefront position of IMF4 is 34, indicating that the time when the fault reaches the N end is 3.4×10^{-5}. According to the ranging formula, the distance among the fault and the head end M is calculated to be 12.06 km. The ranging results of all fault ranging algorithms are shown in Fig. 11.

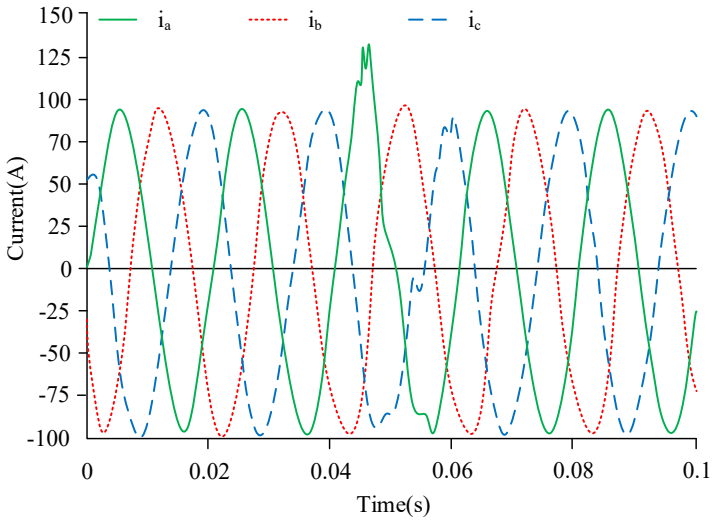

Figure 9: Three-phase current waveform diagram based on ISSA-VMD

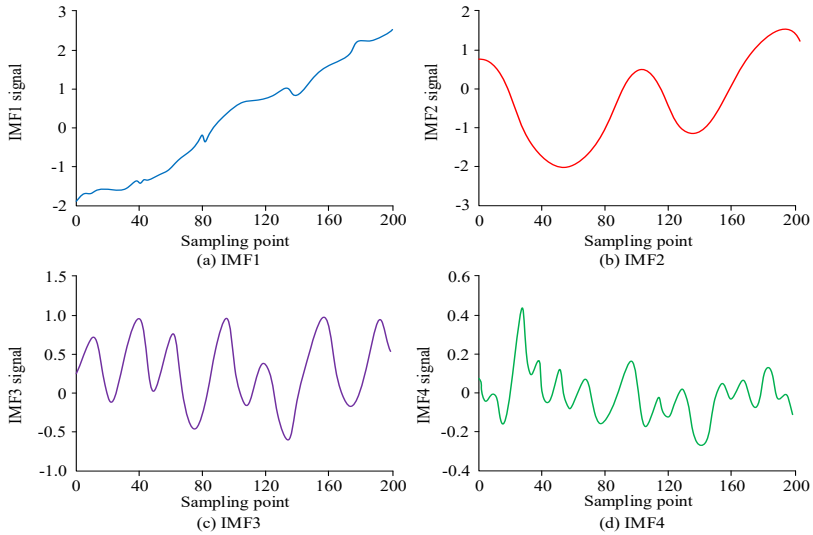

Figure 10: IMF component diagram

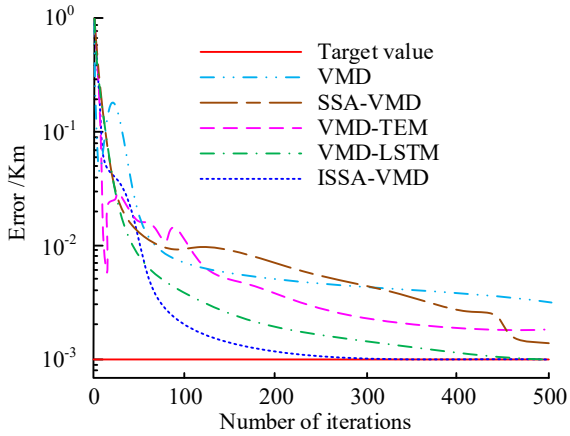

Figure 11: The ranging error result of the fault ranging algorithm

In Figure 11, the fault distance error measured by ISSA-VMD is the smallest, only 0.0010 km. The error distances between VMD and VMD-TEM are relatively large, at 0.0058 km and 0.0031 km. The error distances of SSA-VMD and VMD-LSTM are relatively small, at 0.0027 km and 0.0015 km. The data show that the ISSA-VMD method has the best fault distance measurement effect. To evaluate the performance and robustness of the ISSA-VMD method in an environment close to the actual industrial environment, various tests under complex working conditions are studied and designed. The test is based on a 10kV simulated DNet system, focusing on examining the positioning accuracy of this method under different fault types, fault locations, and transition resistances. The test results are shown in Table 2.

In Table 2, under the ideal conditions without transition resistance (working conditions 1, 2, 5, and 7), the ISSA-VMD method demonstrates extremely high positioning accuracy, with absolute errors all less than 0.01 km and relative errors not exceeding 0.04%. When there is a transition resistance (working conditions 3, 4, and 6), the ranging error increases somewhat, but it is still controlled at a relatively low level. Even at a high transition resistance of 100 Ω (working condition 4), the relative error is only 0.19%, and the absolute error is 0.015 km, fully meeting the precision requirements of engineering applications (usually requiring an error of less than 0.5% or 1%).

For different types of faults, this method maintains stable positioning performance, indicating its good adaptability. To sum up, in the complex tests simulating industrial environments, the average location error of the ISSA-VMD method is 0.007 km (relative error 0.07%), which proves its potential for application in actual DNet fault location and excellent robustness.

Table 2. shows the robustness test results of ISSA-VMD fault location in a simulated industrial environment

Test operating condition number	Fault type	Fault distance (km)	Transition resistance (Ω)	Measurement distance (km)	Absolute error (km)	Relative error (%)
1	Single-phase grounding (AG)	5	0	5.001	0.001	0.02
2	Single-phase grounding (AG)	15	0	14.998	0.002	0.01
3	Single-phase grounding (AG)	12.06	50	12.072	0.012	0.1
4	Single-phase grounding (AG)	8	100	8.015	0.015	0.19
5	Two-phase short circuit (BC)	10	0	9.997	0.003	0.03
6	Two-phase ground contact (BCG)	7.5	10	7.508	0.008	0.11
7	Three-phase short circuit (ABC)	18	0	17.992	0.008	0.04
Statistical results		/	/	Average value	0.007	0.07

4. Discussion

In response to the current shortcomings of SSA, this study improved SSA from 3 aspects: population initialization method, individual PUS formula, and perturbation strategy, and proposed ISSA. ISSA combined with VMD has been applied in DNet TWFL. In the experiment, the initial population distribution of ISSA was more uniform. By improving the introduced RWS, ISSA could overcome the problem of local extremum. Compared to similar algorithms, ISSA also had the best convergence results. For example, the average values of ISSA in Sphere, SumSquares, Ackley, and Griebank were 4.45E-24, 3.95E-37, 2.15E-32, and 1.64E-33. In the same kind of research, LI et al. put forth a TWF single-ended localization method based on VMD and an enhanced energy operator to address the weak distinguishable wavefront problem in the fault reflection wave of a fully parallel autotransformer traction network. This method achieved high fault localization precision [19]. Chen B proposed a GFLS method grounded on ISSA optimization using VMD and multi-scale fuzzy entropy. This method achieved high reliability in most error situations [20]. Compared with Li et al. and Chen et al.'s research, the research method had stronger dynamic adaptability and avoids early convergence to local optima. Experimental results have shown that the distance measurement error of the research method was only 0.001 km, demonstrating superior performance and providing an important reference value for the field of DNet fault detection.

The core engineering value of the proposed ISA-VMD fault location method lies in converting the high-precision algorithm performance into practical power grid operation and maintenance benefits. Firstly, a low error rate of 0.5% (corresponding to a ranging error of 0.001 km) in engineering practice means rapid and precise isolation of the fault point. This can significantly shorten the time for fault detection and repair, reduce the economic losses and social impacts on users caused by power outages, and directly enhance the power supply reliability and quality service level of the DNet. Secondly, ISSA's outstanding global convergence performance and resistance to local optima enable it to demonstrate stronger robustness and adaptability in practical scenarios where the DNet structure is complex and the power flow is variable due to the access of distributed power sources. This means that the approach does not depend on fixed line models or modes of operation. It reduces the workload of on-site debugging and parameter setting, reduces the complexity of technical applications and reliance on the experience of operation and maintenance personnel, and is conducive to promotion in DNets at all levels. Finally, this method automatically finds the optimal parameter combination of VMD through an intelligent optimization algorithm, replacing the manual parameter debugging process that relies on expert experience in traditional methods. This not only improves the automation level of fault location but also provides a feasible technical module for building an intelligent power distribution operation and maintenance management system. In conclusion, the research outcome is not only an improvement in the algorithm but also a potential engineering solution that can directly enhance the safe, reliable, and efficient operation capacity of the DNet.

5. Conclusions

The increasing demand for electricity and the increasing complexity of DNet make TWFL technology is essential in the power system. To overcome the shortcomings of traditional SSA, this study proposes an ISSA. This algorithm enhances its search capability by introducing Torus sequences for population initialization, optimizing individual PUS formulas, and introducing RWS. In addition, combining ISSA with VMD to find the optimal combination of modal number and penalty parameters improves the effectiveness of TWS processing. This study verifies through experiments that the method has good fault detection accuracy and response speed, demonstrating good adaptability in complex power grid environments. Although this study has made progress in algorithm performance, there are still some constraints. The parameter settings of ISSA rely on experience and lack systematic optimization methods. In addition, the robustness of the algorithm in handling extremely intricate situations still needs further validation to adapt to various challenges in the actual power grid. Future research can focus on further optimization of algorithms, such as introducing adaptive parameter adjustment mechanisms to improve efficiency and stability. Meanwhile, ISSA can be combined with other advanced signal processing technologies to enhance fault detection capabilities in complex environments.

Acknowledgment

The research is supported by: Science and Technology Project of China Southern Power Grid Corporation (GDKJXM20230734).

References

[1] Paterna G, Lipari G, Traina E, Comparato G, Muratore A, Livreri P, et al. Design of a Low Voltage and High Power Traveling Wave Tube Based on a Sheet-Beam Rectangular Ring-Bar Slow-Wave Structure. IEEE Access, 2024, 12(1): 9062-9069. https://doi.org/10.1109/ACCESS.2024.3353049.

[2] Koller D P, Schirner M, Ritter P. Human connectome topology directs cortical traveling waves and shapes frequency gradients. Nature Communications, 2024, 15(1): 3570-3583. https://doi.org/10.1038/s41467-024-47860-x.

[3] Tang L. Optical solitons perturbation and traveling wave solutions in magneto-optic waveguides with the generalized stochastic Schrödinger–Hirota equation. Optical and Quantum Electronics, 2024, 56(5): 773-185. https://doi.org/10.1007/s11082-024-06669-0.

[4] Saminu S, Xu G, Zhang S, Kader I A E, Aliyu H A, Jabire A H, Ahmed YK, Adamu MJ. Applications of Artificial Intelligence in Automatic Detection of Epileptic Seizures Using EEG Signals: A Review. Artificial Intelligence and Applications, 2023,1(1): 11-25. https://doi.org/10.47852/bonviewAIA2202297.

[5] Jnaneswar K, Rana A S, Thomas M S. DCVD-VMD enabled traveling wave-based fault location in nonhomogenous AC microgrids. IEEE Systems Journal. 2022,17(2):2411-21. https://doi.org/10.1109/JSYST.2022.3217089.

[6] Zhang D, Song X, Tang H, Li Z, Sun J, Peng W. Fault traveling wave detection method of distribution network based on adaptive VMD and WVD. Journal of Electric Power Science and Technology. 2024, 39(2):80-90. https://doi.org/10.19781/j.issn.1673-9140.2024.02.010.

[7] Zeng R, Zhang L, Wu QH. Fault location scheme for multi-terminal transmission line based on frequency-dependent traveling wave velocity and distance matrix. IEEE Transactions on Power Delivery. 2023, 38(6):3980-90. https://doi.org/10.1109/TPWRD.2023.3293998.

[8] Ni W, Chen Q, Guo X, Liu Y. Enhanced securities investment strategy using ISSA–SVM: a hybrid model combining adaptive moving average, support vector machine, and multi-strategy sparrow search algorithm for improved trend tracking and risk adjustment. Discover Applied Sciences, 2025, 7(6): 1-27. https://doi.org/10.1007/s42452-025-07016-y

[9] Wang J, Li YH, Wang D, Chai M. A reliability calculation method based on ISSA-BP neural network. International Journal of Structural Integrity. 2024, 15(6):1249-1267. https://doi.org/10.1108/IJSI-07-2024-0104.

[10] Xue J, Shen B, Pan A. An intensified sparrow search algorithm for solving optimization problems. Journal of Ambient Intelligence and Humanized Computing. 2023,14(7):9173-9189. https://doi.org/10.1007/s12652-022-04420-9.

[11] Wei F, Feng Y, Shi X, Hou K. Improved sparrow search algorithm with adaptive multi-strategy hierarchical mechanism for global optimization and engineering problems. Cluster Computing. 2025, 28(3):1-44. https://doi.org/10.1007/s10586-024-04883-9.

[12] Wang J, Li YH, Wang D, Chai M. A reliability calculation method based on ISSA-BP neural network. International Journal of Structural Integrity. 2024 Nov 25;15(6):1249-67. https://doi.org/10.1108/IJSI-07-2024-0104

[13] Zhou J, Qu Z, Zhan Z. Traveling wave fault location method of transmission line based on CPO-VMD. Journal of Electric Power Science and Technology. 2025;40(2):30-41. https://doi.org/10.19781/j.issn.1673-9140.2025.02.004

[14] Nazeer S K, Mahalakshmi C, rao P K. Fault location and section identification algorithm on multi-terminal transmission lines using DWT. Journal of The Institution of Engineers (India): Series B. 2024 Aug;105(4):855-870. https://doi.org/10.1007/s40031-024-01016-z

[15] Quan R, Liang W, Wang J, Li X, Chang Y. An enhanced fault diagnosis method for fuel cell system using a kernel extreme learning machine optimized with improved sparrow search algorithm. International Journal of Hydrogen Energy, 2024, 50(1): 1184-1196. https://doi.org/10.1016/j.ijhydene.2023.10.019

[16] Xu D, Li C. Optimization of deep belief network based on sparrow search algorithm for rolling bearing fault diagnosis. IEEE Access, 2024, 12(1): 10470-10481. https://doi.org/10.1109/ACCESS.2024.3354794.

[17] Yue Y, Cao L, Lu D, Hu Z, Xu M, Wang S, et al. Review and empirical analysis of sparrow search algorithm. Artificial Intelligence Review, 2023, 56(10): 10867-10919. https://doi.org/10.1007/s10462-023-10435-1.

[18] Awadallah M A, Al-Betar M A, Doush I A, Makhadmeh S N, Al-Naymat G. Recent versions and applications of sparrow search algorithm. Archives of Computational Methods in Engineering, 2023, 30(5): 2831-2858. https://doi.org/10.1007/s11831-023-09887-z.

[19] Gharehchopogh F S, Namazi M, Ebrahimi L, Abdollahzade B. Advances in sparrow search algorithm: a comprehensive survey. Archives of Computational Methods in Engineering, 2023, 30(1): 427-455. https://doi.org/10.1007/s11831-022-09804-w.

[20] Wang M, Cao H, Ai Z, Zhang Q. Fault diagnosis of ship ballast water system based on support vector machine optimized by improved sparrow search algorithm. IEEE Access, 2024, 12(1): 17045-17057. https://doi.org/10.1109/ACCESS.2024.3351171.

[21] Kong F, Song C, Zhuo Y. Vibration fault analysis of hydropower units based on extreme learning machine optimized by improved sparrow search algorithm. Journal of Vibration Engineering & Technologies, 2023, 11(4): 1609-1622. https://doi.org/10.1007/s42417-022-00660-3.

[22] Li Z, Feng Y, Xia Y, Zhang Y, Liu G, Zhang L, et al. Fault localization of fully parallel AT traction network based on VMD-SSDEO. Journal of Electric Power Science and Technology. 2025;40(1):55-66. https://doi.org/10.19781/j.issn.1673-9140.2025.01.006.

[23] Chen B, Sun Y, Song X, Wang B. Regionalized fault line in distribution networks based on an improved SSA-VMD and multi-scale fuzzy entropy. Electrical Engineering. 2023 Dec;105(6):4399-408. https://doi.org/10.1007/s00202-023-01927-y